# Distinctive Photosystem II Photoinactivation and Protein Dynamics in Marine Diatoms[1][W]

**Hongyan Wu, Amanda M. Cockshutt, Avery McCarthy, and Douglas A. Campbell***

Biology Department, Mount Allison University, Sackville, New Brunswick, Canada E4L 1G7 (H.W., D.A.C.); State Key Laboratory of Marine Environmental Science, Xiamen University, Xiamen, Fujian 361005, China (H.W.); and Chemistry and Biochemistry Department, Mount Allison University, Sackville, New Brunswick, Canada E4L 1G8 (A.M.C., A.M.)



Diatoms host chlorophyll *a*/*c* chloroplasts distinct from green chloroplasts. Diatoms now dominate the eukaryotic oceanic phytoplankton, in part through their exploitation of environments with variable light. We grew marine diatoms across a range of temperatures and then analyzed their PSII function and subunit turnover during an increase in light to mimic an upward mixing event. The small diatom *Thalassiosira pseudonana* initially responds to increased photoinactivation under blue or white light with rapid acceleration of the photosystem II (PSII) repair cycle. Increased red light provoked only modest PSII photoinactivation but triggered a rapid clearance of a subpool of PsbA. Furthermore, PsbD and PsbB content was greater than PsbA content, indicating a large pool of partly assembled PSII repair cycle intermediates lacking PsbA. The initial replacement rates for PsbD (D2) were, surprisingly, comparable to or higher than those for PsbA (D1), and even the supposedly stable PsbB (CP47) dropped rapidly upon the light shift, showing a novel aspect of rapid protein subunit turnover in the PSII repair cycle in small diatoms. Under sustained high light, *T. pseudonana* induces sustained nonphotochemical quenching, which correlates with stabilization of PSII function and the PsbA pool. The larger diatom *Coscinodiscus radiatus* showed generally similar responses but had a smaller allocation of PSII complexes relative to total protein content, with nearly equal stiochiometries of PsbA and PsbD subunits. Fast turnover of multiple PSII subunits, pools of PSII repair cycle intermediates, and photoprotective induction of nonphotochemical quenching are important interacting factors, particularly for small diatoms, to withstand and exploit high, fluctuating light.

Diatoms are oxygenic photoautotrophs whose cell structures and chlorophyll *a*/*c* chloroplasts are evolutionarily, structurally, and functionally distinct from the green lineage with chlorophyll *a*/*b* chloroplasts (Armbrust et al., 2004; Wilhelm et al., 2006; Larkum et al., 2007). Over the past 100 million years (Bowler et al., 2010), diatoms have become nearly ubiquitous, accounting for approximately 20% of global primary productivity (Field et al., 1998). They are currently by far the most successful group of eukaryotic phytoplankton, not only in terms of primary production but also in their number of species (Medlin and Kaszmarska, 2004), which span a wide cell size range (Beardall et al., 2009). Therefore, diatoms functionally dominate the phytoplankton population (Wilhelm et al., 2006), particularly in turbulent coastal waters where they are exposed to frequent and large fluctuations in light due to fast vertical mixing through steep photic zone light gradients (Long et al., 1994; MacIntyre et al., 2000).

In response to a sudden increase in irradiance, diatoms can dissipate excess light energy through distinct mechanisms of nonphotochemical quenching (NPQ; Lavaud et al., 2004; Eisenstadt et al., 2008; Grouneva et al., 2009; Bailleul et al., 2010; Park et al., 2010; Zhu and Green, 2010) to limit overexcitation of their photosystems, including mechanisms for sustained conversion of PSII units to a down-regulated state. Overexcitation of PSII can lead to the production of reactive oxygen species (ROS; Müller et al., 2001), causing damage to the photosynthetic apparatus (Nishiyama et al., 2006) and leading potentially to cell death (Janknegt et al., 2009). Diatoms, like all oxygenic photoautotrophs, are subject to photoinactivation of their PSII reaction centers (Nagy et al., 1995; Six et al., 2007; Edelman and Mattoo, 2008). To maintain photosynthesis, the cells must counter the photoinactivation of PSII with repair through proteolytic removal of photodamaged proteins (Silva et al., 2003; Nixon et al., 2010) and the coordinated insertion of newly synthesized subunits into the thylakoid membrane (Aro et al., 1993). If photoinactivation outruns the rate of repair, the PSII pool suffers net photoinhibition (Aro et al., 2005; Nishiyama et al., 2005, 2006; Murata et al., 2007), leading ultimately to a decrease in photosynthetic capacity. Thus, the risks of upward fluctuations

[1] This work was supported by the Natural Sciences and Engineering Research Council of Canada (to D.A.C.), the Canada Foundation for Innovation (to D.A.C.), the New Brunswick Innovation Foundation (to D.A.C. and A.M.C.), and AgriSera (to A.M.C.).

* Corresponding author; e-mail dcampbell@mta.ca.

The author responsible for distribution of materials integral to the findings presented in this article in accordance with the policy described in the Instructions for Authors (www.plantphysiol.org) is: Douglas A. Campbell (dcampbell@mta.ca).

[W] The online version of this article contains Web-only data.
www.plantphysiol.org/cgi/doi/10.1104/pp.111.178772

in irradiance constitute a potent selective pressure contributing to niche partitioning among different phytoplankton species (Six et al., 2007).

Key et al. (2010) found that under moderately high blue light (BL), diatoms have a low intrinsic susceptibility to photoinactivation of PSII when compared with picoprokaryotes, such as *Prochlorococcus* and *Synechococcus* (Six et al., 2007), the prasinophyte chlorophyll *a*/*b* green alga *Ostreococcus* (Six et al., 2009), the chlorophyll *a*/*c* eukaryote *Pelagococcus*, or the rhodophyte phytoplankton *Porphyridium* (D.A. Campbell, C. Six, and L. Dubois, unpublished data). Furthermore, metabolic PSII repair shows a negative correlation with cell size across two genera of representative centric and multicentric marine diatoms (Key et al., 2010). The unstable character of PSII has been conserved throughout evolution across oxygenic photoautotrophs (Critchley et al., 1992; Kim et al., 1993; Sundby et al., 1993; Mattoo et al., 1999; Edelman and Mattoo 2008). In model cyanobacteria, green algae, and higher plants under illumination, the turnover of PsbA (D1) protein encoded by the *psbA* gene is significantly faster than the turnover of other PSII subunits, such as the PsbD (D2) and PsbB (CP47) proteins (de Vitry et al., 1989; Yu and Vermaas, 1990; Zhang et al., 1999; Komenda et al., 2004; Edelman and Mattoo, 2008; Yao et al., 2009; Nixon et al., 2010). Therefore, the PSII repair cycle is often discussed primarily in terms of the proteolytic removal and replacement of the D1 subunit of PSII (Silva et al., 2003; Komenda et al., 2004; Nixon et al., 2010), with the implicit or explicit assumption that turnover rates of the other PSII subunits are consistently slower, although exceptions have been noted (Baroli and Melis, 1996). To our knowledge, rates of PSII subunit turnover have not been measured in diatoms, which thrive under variable light (Nymark et al., 2009) and whose chlorophyll *a*/*c* chloroplasts are functionally and structurally distant from chlorophyll *a*/*b* chloroplasts (Wilhelm et al., 2006; Larkum et al., 2007). Here, we quantitatively analyze PSII function and protein subunit turnover in representative morphologically centric marine diatoms, *Thalassiosira pseudonana* and *Coscinodiscus radiatus*, treated with light challenges to understand whether distinct PSII dynamics in their chlorophyll *a*/*c* chloroplasts contribute to the strong diatom capacity for exploitation of variable light.

## RESULTS

### Photoinhibition of the Photochemical Yield of PSII

We grew *T. pseudonana* and *C. radiatus* cells under 30 $\mu$mol photons $m^{-2}$ $s^{-1}$, a light level equivalent to the bottom 10% of the photic zone depth. To assess their capacities to then exploit variable light, we challenged them with a 90-min shift to 450 $\mu$mol blue photons $m^{-2}$ $s^{-1}$, equivalent to a rapid mixing event to a light field approximating the upper third of the photic zone, or to 1,400 $\mu$mol white photons $m^{-2}$ $s^{-1}$, a light field approximating the top 7% of the photic zone. We also exposed cells to a red light (RL) challenge of 450 $\mu$mol red photons $m^{-2}$ $s^{-1}$. Although this RL field is of limited ecophysiological relevance to typical water columns, the comparison with responses under BL promised mechanistic insights, since both RL and BL are photosynthetically active but the quantum yield for photoinactivation is much higher under BL (Sarvikas et al., 2006). After the light challenge, we shifted cells back to their original low growth light to track recovery processes.

In *T. pseudonana* and *C. radiatus* cells maintaining a PSII repair cycle, the maximum photochemical yield of PSII, measured by the ratio $F_v/F_m$, initially dropped during the 90-min RL, BL, or white (WL) high-light exposures (Fig. 1, white symbols) but stabilized and then recovered either late in the high-light period (RL) or during the subsequent growth light period (BL and WL). When the PSII repair cycle was blocked by the addition of lincomycin (Fig. 1, black symbols), moderate RL provoked a modest decrease in $F_v/F_m$, while

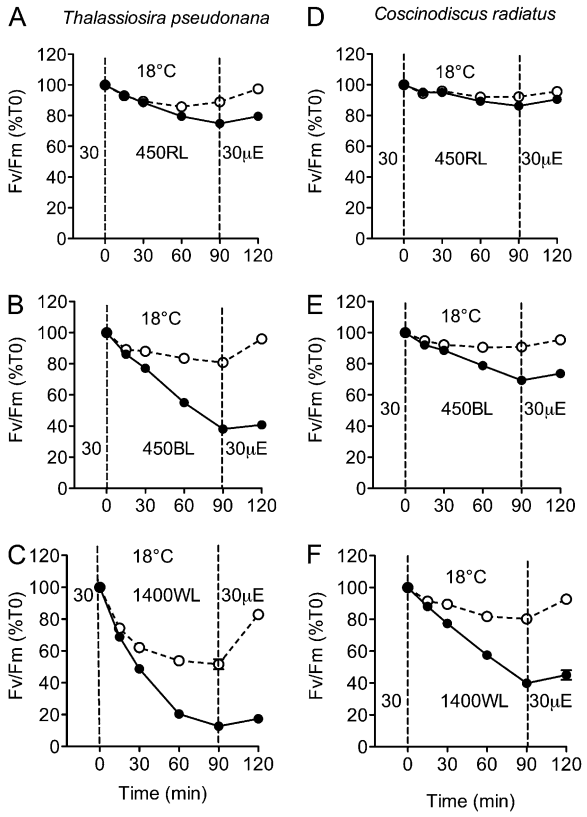


**Figure 1.** Responses of $F_v/F_m$ versus time in *T. pseudonana* (A–C) and *C. radiatus* (D–F) cultures treated with (black symbols) or without (white symbols) the chloroplast protein synthesis inhibitor lincomycin. Both species were grown at 18°C and 30 $\mu$mol photons $m^{-2}$ $s^{-1}$, exposed to 450 $\mu$mol photons $m^{-2}$ $s^{-1}$ RL (A and D) or BL (B and E) or 1,400 $\mu$mol photons $m^{-2}$ $s^{-1}$ WL (C and F) for 90 min, and then allowed to recover at 30 $\mu$mol photons $m^{-2}$ $s^{-1}$ for 30 min. $n = 4$ to 5 independent culture experiments; error bars represent SE, although most of them are within symbols.

moderate BL or the high-level WL provoked significant declines in $F_v/F_m$.

Diatoms have significant capacities to induce phases of NPQ, which lower the achieved photochemical yield of PSII. Supplemental Figure S1 plots the dynamic NPQd phase, which relaxes within 5 min of dark incubation and is reinduced during a brief exposure to the treatment light. In control cells that maintained steady pools of active PSII, this NPQd phase varied only modestly across the period of exposure to high-light treatment. In contrast, in the cells that lost PSII activity when treated with lincomycin and were exposed to elevated BL (Fig. 1B) or WL (Fig. 1, C and F), the NPQd dropped approximately in parallel with the loss of PSII activity (Supplemental Fig. S1, B, C, and F). Thus, maintaining PSII maximum quantum yield is required to maintain capacity for dynamic regulation of NPQd.

Figure 2 plots the sustained NPQs phase, which is induced over the period of high-light treatment and which is sustained through the 5-min dark period that immediately precedes measurements. NPQs, by definition, starts at 0, since it uses the initial level of $F_m$ as the baseline for subsequent measures. Cells that suffered significant drops in PSII activity under BL in the presence of lincomycin (Fig. 2, B and E) or particularly under high WL without or with lincomycin (Fig. 2, C and F) showed a large induction of this NPQs phase, which relaxed in part during the subsequent 30-min recovery incubation at growth light. Given the unfolding complexities of NPQ in diatoms, we are not assigning a mechanistic interpretation to this sustained phase of NPQs. NPQs does accumulate and subsequently relax even when chloroplastic protein synthesis is blocked and so is distinct from the classic qi inhibition quenching mechanism.

Given the evidence for the induction of sustained NPQs, to partition the influences of PSII photoinactivation from the influences of NPQs on PSII photochemical yield, in Supplemental Figure S2 we plot the parameter $1/F_0 - 1/F_m$ (Havaux et al., 1991), which has been linearly correlated with the content of functional PSII complexes (Park et al., 1995; Lee et al., 1999). Ideally we would have in parallel measured oxygen flash yields to track functional PSII content, but those measurements were not feasible on the time scales required for these time-course experiments. Under moderate RL, the smaller *T. pseudonana* showed a moderate drop in $1/F_0 - 1/F_m$ in the presence of lincomycin, reflecting some net photoinactivation of PSII, while in control cells with an active PSII repair cycle, $1/F_0 - 1/F_m$ was almost steady across the light treatment (Supplemental Fig. S2A), with the PSII repair cycle almost fully countering the underlying PSII photoinactivation. The larger *C. radiatus* suffered only moderate net photoinactivation under moderate RL, but there was little difference between cells with or without lincomycin (Supplemental Fig. S2D), therefore showing little induction of PSII repair to counter the moderate PSII photoinactivation. Recall that under

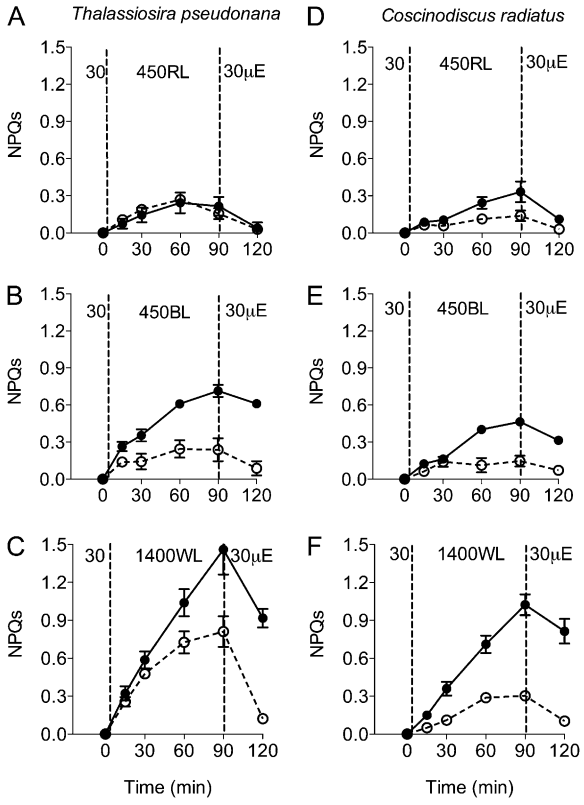


**Figure 2.** Responses of NPQs [$(F_{mt0} - F_m)/F_m$] versus time in *T. pseudonana* (A–C) and *C. radiatus* (D–F) cultures treated with (black symbols) or without (white symbols) the chloroplast protein synthesis inhibitor lincomycin to block PSII repair. Both species were grown at 18°C and 30 $\mu$mol photons $m^{-2}$ $s^{-1}$, exposed to 450 $\mu$mol photons $m^{-2}$ $s^{-1}$ RL (A and D) or BL (B and E) or 1,400 $\mu$mol photons $m^{-2}$ $s^{-1}$ WL (C and F) for 90 min, and then allowed to recover at 30 $\mu$mol photons $m^{-2}$ $s^{-1}$ for 30 min. $n = 4$ to 5 separate culture experiments; error bars represent SE, although most of them are within symbols.

these RL treatments, there was only limited induction of sustained NPQs in either *T. pseudonana* or *C. radiatus* (Fig. 2, A and D). In both species under moderate BL, $1/F_0 - 1/F_m$ declined in cells with lincomycin, but cells without lincomycin were able to limit the drop in $1/F_0 - 1/F_m$, which stabilized from 30 min onward (Supplemental Fig. S2, B and E). Recall that under the BL treatment, cells with lincomycin induced significant sustained NPQs (Fig. 2, B and E).

The high-WL treatment provoked an intriguing biphasic response in the PSII parameter $1/F_0 - 1/F_m$, particularly in *T. pseudonana* (Supplemental Fig. S2, C and F). During the first 30 min of high WL, $1/F_0 - 1/F_m$ dropped sharply in cells both without and with lincomycin, as rapid photoinactivation outran the induction of PSII repair. After 30 min, however, $1/F_0 - 1/F_m$ nearly stabilized in *T. pseudonana* (Supplemental Fig. S2C). This stabilization coincides with a massive induction of NPQs (Fig. 2C). The pattern in *C. radiatus* under high white light was similar (Supplemental Fig. S2F), although the induction of NPQs was smaller (Fig. 2F).

Upon a moderate upward shift in light (Key et al., 2010), the smaller *T. pseudonana* relied upon induction of PSII repair to counter photoinactivation, shown by the divergence between the treatments without and with lincomycin (Supplemental Fig. S2, A and B). In contrast, under the same moderate upward light shifts, the larger *C. radiatus* showed less reliance upon induction of PSII repair, with less divergence between cells treated with or without lincomycin (Supplemental Fig. S2, D and E). Under stronger light (Supplemental Fig. S2, C and F) or in the presence of lincomycin when PSII function was dropping (Supplemental Fig. S2B), *T. pseudonana*, and to an extent *C. radiatus*, induced a sustained phase of NPQs, which coincided with stabilization of the PSII parameter $1/F_0 - 1/F_m$, even in the presence of lincomycin (Supplemental Fig. S2C).

When the cells were returned to the growth light level of 30 $\mu$mol $m^{-2}$ $s^{-1}$, they showed significant recovery in $F_v/F_m$ within 30 min (Fig. 1). The recovery observed in the control samples can be attributed to both PSII repair and relaxation of NPQ processes, whereas the limited recovery in the lincomycin-treated samples is attributed to the slow relaxation of NPQs, because PSII repair was blocked. This distinction between relaxation of NPQs and PSII repair is shown in the $1/F_0 - 1/F_m$ plots, where cells with lincomycin showed no recovery but cells with active PSII repair cycles did show some recovery (Supplemental Fig. S2, C, E, and F).

### Effective Target Size for PSII Photoinactivation, and Functional Absorbance Cross Section for PSII and PSII Repair Rates

We extracted an effective target size for photoinactivation of PSII ($\sigma_i$ [units of $Å^2$ $quanta^{-1}$]; Six et al., 2007; Campbell and Tyystjärvi, 2011), equivalent to a rate constant for photoinactivation, $k_{PI}$ (Kok, 1956), generalized across light levels by division by the incident photon flux density (Oliver et al., 2003). We estimated $\sigma_i$ from the decrease in $1/F_0 - 1/F_m$ plotted versus cumulative incident photons in the absence of PSII repair over the 90-min moderate light exposures to RL or BL (Supplemental Fig. S3, A and B) or over the first 30 min of high WL exposure (Supplemental Fig. S3, A and B). Thirty minutes of high WL gave a cumulative photon exposure equivalent to 90 min of the moderate RL or BL. As expected, $\sigma_i$ was larger under BL than under RL (Table I). Under the moderate light treatments, $\sigma_i$ for the smaller diatom *T. pseudonana* was larger than for *C. radiatus*, whether estimated on the basis of the photoinhibition parameter $1/F_0 - 1/F_m$ or on the basis of $F_v/F_m$ as in our earlier determinations (Key et al., 2010). The appropriate data treatment depends upon the goal: plots of $F_v/F_m$ track operational changes in PSII maximum quantum yield, while the plot of $1/F_0 - 1/F_m$ comes closer to separating photoinactivation processes from the influences of sustained NPQs. Changing the growth and treatment temperatures had little effect on $\sigma_i$ (Supplemental Fig. S3, B and D), so primary susceptibility to photoinactivation showed little response to temperature. Under high WL over the first 30 min of exposure the $\sigma_i$, susceptibility to photoinactivation was intermediate between the levels for RL and BL. Thereafter, however, the cells under strong WL showed near stabilization of the photoinhibition parameter $1/F_0 - 1/F_m$, so the $\sigma_i$ estimates became very small. Note that the $F_v/F_m$ measure continues to decline under the extended strong WL exposure (Fig. 1, C and F) through the combined influence of NPQs and photoinactivation. Figure 3 plots time-resolved estimates for the PSII photoinactivation rate, showing that the accumulation of NPQs under sustained incubation correlates with a decrease in photoinactivation rate, particularly under high WL.

During exponential growth conditions, *T. pseudonana* showed a larger functional absorbance cross section for PSII photochemistry ($\sigma_{PSII}$) than did *C. radiatus*

**Table I.** *Photophysiological properties of T. pseudonana and C. radiatus exposed to moderately high RL, BL, and WL*

$\sigma_i$ was estimated on the basis of changes in the PSII parameter $1/F_0 - 1/F_m$ to partition PSII photoinactivation from the influence from sustained phases of NPQ. $n$ = 4 to 5 independent culture experiments; SE values are given in parentheses.

| Parameter | Species | Light Treatment | | | | |
|---|---|---|---|---|---|---|
| | | RL (450 $\mu$mol $m^{-2}$ $s^{-1}$) | BL (450 $\mu$mol $m^{-2}$ $s^{-1}$) | | | WL (1,400 $\mu$mol $m^{-2}$ $s^{-1}$) |
| | | 18°C | 12°C | 18°C | 24°C | 18°C |
| $\sigma_i$ ($Å^2$ $quanta^{-1}$) | *T. pseudonana* | $3.5 \times 10^{-5}$ ($0.1 \times 10^{-5}$) | $7.2 \times 10^{-5}$ ($0.2 \times 10^{-5}$) | $8.8 \times 10^{-5}$ ($0.4 \times 10^{-5}$) | $8.1 \times 10^{-5}$ ($0.2 \times 10^{-5}$) | $6.7 \times 10^{-5}$[a] ($0.2 \times 10^{-5}$) |
| | *C. radiatus* | $2.6 \times 10^{-5}$ ($0.2 \times 10^{-5}$) | | $5.8 \times 10^{-5}$ ($0.3 \times 10^{-5}$) | $6.7 \times 10^{-5}$ ($0.4 \times 10^{-5}$) | $3.9 \times 10^{-5}$[a] ($0.3 \times 10^{-5}$) |
| $\sigma_{PSII}$ ($Å^2$ $quanta^{-1}$) | *T. pseudonana* | | 247.5 (5.0) | 257.2 (2.6) | 260.0 (4.0) | |
| | *C. radiatus* | | | 147.3 (4.3) | 143.4 (7.1) | |
| $\sigma_{PSII}/\lvert\sigma_i\rvert$ | *T. pseudonana* | | $2.9 \times 10^7$ | $3.4 \times 10^7$ | $3.13 \times 10^7$ | |
| | *C. radiatus* | | | $3.9 \times 10^7$ | $4.7 \times 10^7$ | |

[a]$\sigma_i$ fits for WL treatments taken from the first 30 min of treatment, giving cumulative photon doses equivalent to 90 min of treatment under RL or BL.

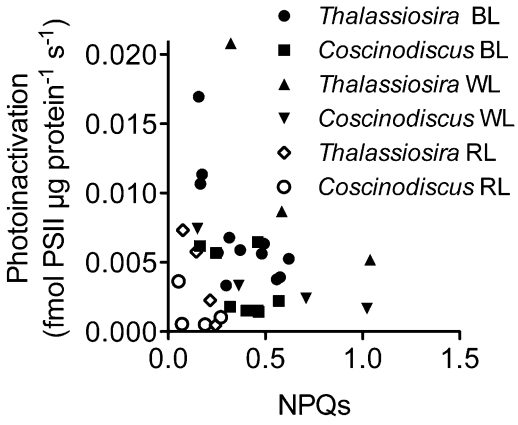


**Figure 3.** Negative correlation of the PSII photoinactivation rate with induction of NPQs. Time-resolved PSII photoinactivation rate was estimated for each measurement interval during exposure to RL, BL, or high WL. NPQs was measured for the same measurement interval. $n$ = 4 to 5 separate culture experiments for each data point; error bars on individual treatment/time points were omitted for clarity.

(Table I). To estimate the deliveries of excitons to PSII per round of photoinactivation, we calculated the ratio of $\sigma_{PSII}$ to $\sigma_i$ (Table I) for BL, the condition for which we have estimates of both $\sigma_{PSII}$ and $\sigma_i$ . In *T. pseudonana*, $\sigma_{PSII}/|\sigma_i|$ was about 74% of the value in *C. radiatus*, indicating fewer rounds of photochemical charge separation per round of PSII repair in *T. pseudonana*, which suffers more frequent photoinactivations.

### Accumulation of Malondialdehyde Content as an Index of Cumulative ROS Toxicity

For *T. pseudonana* and *C. radiatus* under RL, BL, and WL treatments, no significant additional accumulation of malondialdehyde (MDA) was induced after 90 min of exposure when compared with the initial level at time 0 (Fig. 4) in cells without or with lincomycin. The larger *C. radiatus* contained somewhat higher levels of MDA, expressed relative to total protein content, under growth conditions at time 0. For cells grown and treated at 12°C or 24°C, results were similar (data not shown). Therefore, our treatments did not appear to provoke significant cumulative ROS toxicity.

### Quantitation of PSII Subunit Levels under Increased Light

We quantified the levels and variation in the content of key PSII proteins PsbA (D1; Fig. 5), PsbD (D2; Supplemental Fig. S4), and PsbB (CP47; Supplemental Fig. S5) during the 90-min high-light exposure and the subsequent 30-min recovery under RL, BL, and WL treatments. For *T. pseudonana* under RL, PsbA content (Fig. 5A) dropped only marginally in the control cells after 90 min of exposure, whereas the lincomycin-treated cells showed an initial fast drop in PsbA content to 68% of time 0 within the first 30 min, with steady levels thereafter. BL induced no significant change of PsbA content in the control cells (Fig. 5B), but in the presence of lincomycin it led to a progressive drop in PsbA to 68% of time 0 by the end of the 90-min high-light treatment. WL drove a significant drop of PsbA in the control cells (Fig. 5C) and a bigger drop in the lincomycin-treated cells. In contrast, high-light treatments (RL, BL, and WL; Fig. 5, D–F) did not cause any net loss of PsbA in the control cells of *C. radiatus*; on the contrary, PsbA content had increased by the 90-min point. The lincomycin-treated *C. radiatus* cells showed a net decline of PsbA content during the high-light exposure, but to a lesser extent than in *T. pseudonana* under comparable treatments. Patterns of PsbA protein content in cells grown and treated at 12°C and 18°C were similar (data not shown).

For *T. pseudonana*, high RL did not provoke changes in the content of PsbD, either with or without lincomycin (Supplemental Fig. S4A). In marked contrast, under BL treatment, PsbD dropped sharply during the first 15 min in the lincomycin-treated cells (Supplemental Fig. S4B). WL resulted in a significant loss of PsbD for the first 30 min in cells both with and without lincomycin (Supplemental Fig. S4C); after that, the

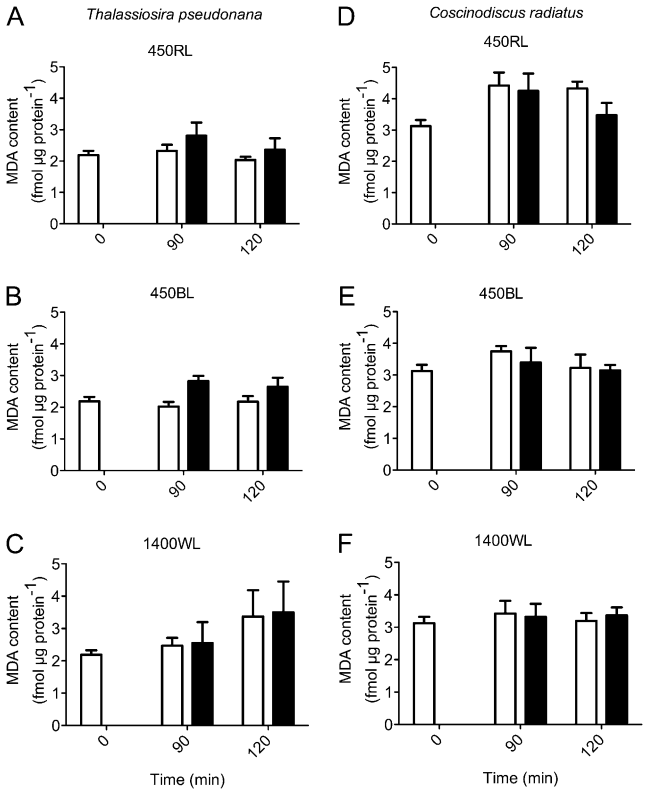


**Figure 4.** Changes in MDA content, a product of ROS peroxidation of membrane lipids, in *T. pseudonana* (A–C) and *C. radiatus* (D–F) cultures treated with (black bars) or without (white bars) the chloroplast protein synthesis inhibitor lincomycin after exposure to high RL, BL, or WL for 90 min and the subsequent 30-min recovery at growth light. $n$ = 4; error bars represent SE.

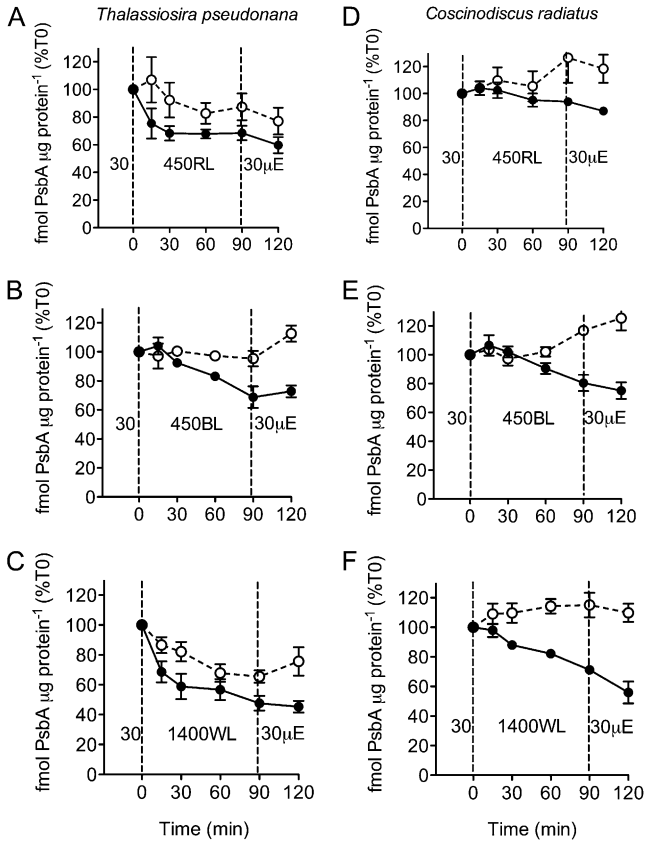


**Figure 5.** Changes in PsbA content in *T. pseudonana* (A–C) and *C. radiatus* (D–F) cultures treated with (black symbols) or without (white symbols) the chloroplast protein synthesis inhibitor lincomycin. Both species were grown at 30 $\mu$mol photons $m^{-2}$ $s^{-1}$, exposed to 450 $\mu$mol photons $m^{-2}$ $s^{-1}$ RL or BL or 1,400 $\mu$mol photons $m^{-2}$ $s^{-1}$ WL for 90 min, and then allowed to recover at 30 $\mu$mol photons $m^{-2}$ $s^{-1}$ for 30 min. $n = 3$; error bars represent SE.

PsbD content stabilized in cells without lincomycin. The variations of PsbD content in *C. radiatus* during the high-light exposures (Supplemental Fig. S4, D–F) were similar to those in *T. pseudonana*, but *C. radiatus* generally showed larger differences between cells with and without lincomycin.

For *T. pseudonana*, elevated RL did not provoke changes in the content of PsbB content, either with or without lincomycin (Supplemental Fig. S5A). In contrast, elevated BL or WL did result in declines in PsbB content, particularly in the presence of lincomycin. In contrast, *C. radiatus* (Supplemental Fig. S5, D–F) showed a distinct accumulation of PsbB content upon a shift to increased light, which was blocked by the addition of lincomycin.

### Comparisons of Protein Subunit Turnover and PSII Function

In both *T. pseudonana* (Figs. 5A and 6A) and *C. radiatus* (Figs. 5D and 6D), a shift to increased RL provoked a significant initial drop in PsbA protein content in the presence of lincomycin. There were only small changes in $1/F_0 - 1/F_m$ (or indeed in $F_v/F_m$) during these RL treatments. Elevated BL (Fig. 6, B and E) and high WL treatments (Fig. 6, C and F) provoked significant drops in $1/F_0 - 1/F_m$ with approximately proportional and progressive drops in PsbA, particularly in *T. pseudonana* (Fig. 6B).

In *T. pseudonana* grown under low light at 12°C, 18°C, or 24°C and then shifted to elevated light (Fig. 7A), the changes in molar content of PsbD and PsbA were similar in magnitude and rate. To our surprise, PsbD started from a higher initial content, indicating a large initial excess of PsbD (and also PsbB subunits; data not shown) over PsbA subunits in the *T. pseudonana* growing under low to moderate light. This excess pool of PsbD (and PsbB) persisted even under strong photoinhibition, with a residual pool of 37 ± 7 fmol PsbD $\mu g^{-1}$ protein even when PsbA $\mu g^{-1}$ protein is extrapolated to 0 (Fig. 7A). In *C. radiatus*, in contrast, initial contents of PsbD and PsbA were similar, as expected from the 1:1 ratio of these subunits in the assembled PSII complex. Note that the overall allocations

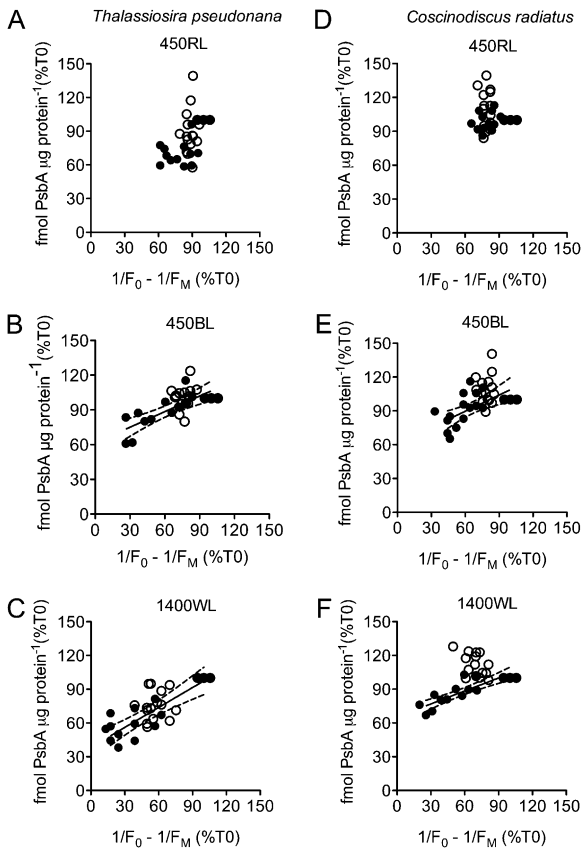


**Figure 6.** Change in PsbA content versus photoinhibition ($1/F_0 - 1/F_m$) in *T. pseudonana* (A–C) and *C. radiatus* (D–F) cultures during a 90-min exposure to high RL, BL, and WL and subsequent recovery at growth light. The data from the cultures treated with lincomycin (black symbols) and without lincomycin (white symbols) were pooled for the regression fit. $n = 3$ independent cultures; dashed lines indicate 95% confidence intervals for the regression curves.

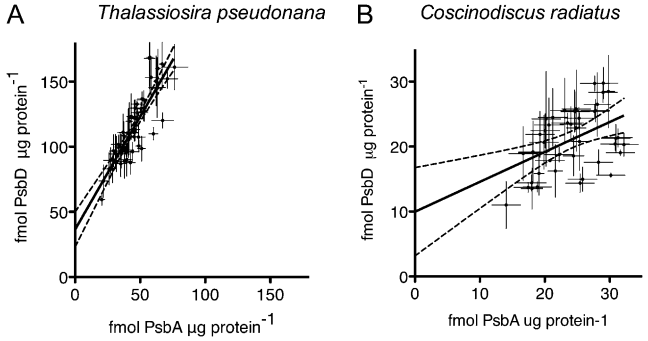


**Figure 7.** PsbD content versus PsbA content in *T. pseudonana* (A) and *C. radiatus* (B) cultures grown at 12°C, 18°C, or 24°C treated with or without the chloroplast protein synthesis inhibitor lincomycin over a 90-min exposure to high RL, BL, or WL and subsequent recovery at growth light. $n = 3$; average data from each condition and time point are plotted with SE. Dashed lines indicate 95% confidence intervals for the regression curves. For *T. pseudonana*, slope = 1.7 ± 0.14, *y* intercept = 37 ± 6.7 fmol PsbD $\mu g^{-1}$ protein, and $r^2 = 0.74$; for *C. radiatus*, slope = 0.5 ± 0.1, *y* intercept = 10 ± 3.4 fmol PsbD $\mu g^{-1}$ protein, and $r^2 = 0.2$. Note the different axis scales between A and B.

to PsbA and PsbD in *C. radiatus* were significantly lower than in *T. pseudonana* when expressed on the basis of total protein. In *C. radiatus* shifted to elevated RL, BL, or WL, PsbA and PsbD changed to similar extents (Fig. 7B), although with scatter among the different light treatments and growth temperatures. Overall, in both *T. pseudonana* and *C. radiatus* shifted to elevated light, the PsbD protein subunit showed turnover properties similar to PsbA (Figs. 5 and 7; Supplemental Fig. S4). Changes in PsbB were smaller, but even this supposedly stable subunit showed significant and rapid changes in content upon the shift to elevated light (Supplemental Fig. S5).

To compare the turnover of protein subunits and the regeneration of functional PSII complexes after photoinactivation, we estimated pool sizes for key intermediate stages of the PSII repair cycle, photoinactivation rates, and PSII repair rates for the regeneration of active PSII centers from precursor pools (Fig. 8). We present these estimates for the shift from low growth light to moderately high BL. *T. pseudonana* growing under low light contained about 43 fmol active PSIIa centers $\mu g^{-1}$ protein (Fig. 8A), estimated as the initial pool of 47 fmol PsbA $\mu g^{-1}$ protein minus a pool of 4 fmol PsbA $\mu g^{-1}$ protein that was cleared without a compensatory drop in $1/F_0 - 1/F_m$ (or in $/F_v/F_m$) upon a shift to elevated RL (Fig. 5A; compare Supplemental Fig. S3A). We assigned this 4 fmol PsbA $\mu g^{-1}$ protein pool to intact but inactive PSIIi centers that are present in the low-light cells but rapidly cleared upon a shift to RL. These low-light *T. pseudonana* cells also contained about 120 fmol PsbD $\mu g^{-1}$ protein, giving a pool of 78 fmol PsbD $\mu g^{-1}$ protein, in excess above the content of total PsbA. We assigned this large pool to disassembled PSIId, pools of PSII repair cycle intermediates. Under this initial low-light condition, the rate of photoinactivation converting active to inactive PSIIi was $7 \times 10^{-4}$ PSII $\mu g^{-1}$ protein $s^{-1}$ and was fully countered by a slow repair rate, converting disassembled to active PSIIa, to maintain stable $F_v/F_m$ and $1/F_0 - 1/F_m$.

Upon a shift to increased BL (Fig. 8A) or WL (data not shown), the *T. pseudonana* cells suffered photoinhibition of PSII activity and changes in the pools of PSII repair cycle intermediates. Upon shifting upward to a moderately high BL field, 15× higher than the growth light, the photoinactivation rate increased sharply to $1 \times 10^{-2}$ PSII $\mu g^{-1}$ protein $s^{-1}$ (Fig. 8B). The induction of PSII repair lagged, but by 30 min of increased BL, the rate of photoinactivation fell back to $6 \times 10^{-3}$ PSII $\mu g^{-1}$ protein $s^{-1}$ and the induction of PSII repair (Fig. 8B) was sufficient to generate newly assembled active PSII (Fig. 8A) to counter the photo-

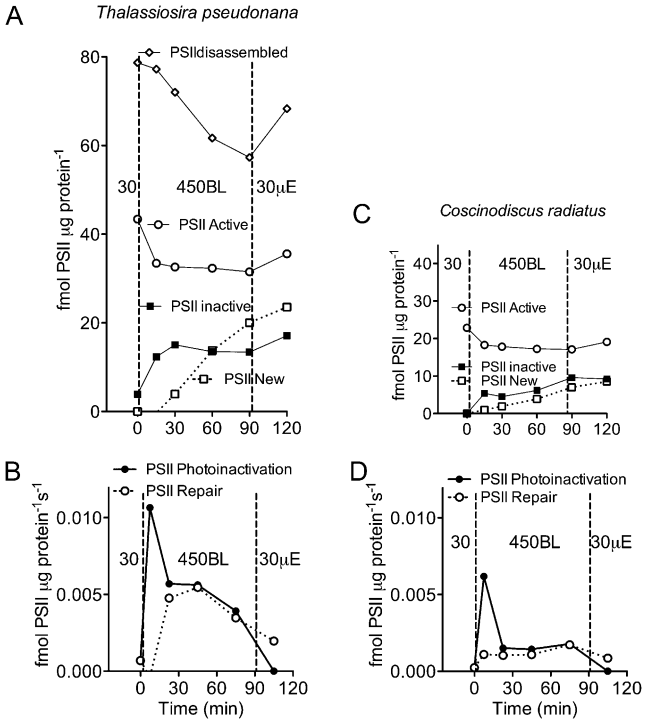


**Figure 8.** PSII repair cycle intermediate pools, photoinactivation rates, and repair rates in *T. pseudonana* (A and B) and *C. radiatus* (C and D) shifted from low growth light to higher BL, provoking moderate photoinhibition of PSII activity. Pool size estimates are expressed in fmol $\mu g^{-1}$ protein, estimated based on analyses of levels and changes in PsbA and PsbD protein pools (Fig. 5; Supplemental Fig. S4), in comparison with changes in PSII activity ($1/F_0 - 1/F_m$; Fig. 4). The time-resolved rate of PSII photoinactivation was estimated as the change in $1/F_0 - 1/F_m$ over a given measurement interval multiplied by the content of active PSII at the start of the time interval. For the initial growth light condition at time 0, PSII activity was stable over time, so the rate of PSII repair was set equal in magnitude to the rate of photoinactivation, estimated as $\sigma_i$ ($m^2$ $quanta^{-1}$) × photosynthetic photon flux density (quanta $m^{-2}$ $s^{-1}$) × content of active PSII. For the high-light condition, time-resolved PSII repair was estimated for each measurement interval as the change in active PSII content in the absence of lincomycin (PSII repair active) minus the change in active PSII content in the presence of lincomycin (PSII repair blocked).

inactivation rate, leading to stabilization of PSII function, albeit at a lower level of 32 fmol active PSII centers $\mu g^{-1}$ protein (Fig. 8A). This stabilization coincided with the induction of sustained NPQs (Fig. 2B). During the elevated blue exposure, the estimated pool of disassembled PSII declined by about one-third, from 78 to 57 fmol PSII $\mu g^{-1}$ protein. Thus, the cells drew down their initial pools of disassembled PSIId units to support a rapid acceleration in PSII repair, sufficient to counter the photoinactivation rate. Overall, this drawdown of repair cycle intermediates led to a moderate drop in the overall content of PSII units under elevated BL. The patterns of PSII repair cycle intermediates under higher WL were similar, although the induction of NPQs was stronger, the down-regulation of PSII photoinactivation was more marked (data not shown), and the induction of PSII repair was slower and weaker.

When compared with *T. pseudonana*, *C. radiatus* growing under low light showed a different pattern of PSII repair cycle intermediates (Fig. 8C). *C. radiatus* contained only 23 fmol active PSIIa units $\mu g^{-1}$ protein, about half the allocation in *T. pseudonana*. More strikingly, *C. radiatus* showed no evidence for the pool of intact but inactive PSIIi centers found in low-light *T. pseudonana*. The molar ratio of PsbD:PsbA was close to 1 under low-light growth and remained close to 1 during the elevated light treatments, as expected from the stoichiometric composition of PSII complexes. Therefore, we found no evidence for significant pools of disassembled PSII repair cycle intermediates in *C. radiatus* under any of the tested conditions. The smaller pool of PSII in *C. radiatus* suffered a slower low-light photoinactivation rate, at only $2.4 \times 10^{-4}$ PSII $\mu g^{-1}$ protein $s^{-1}$, which was again fully countered by a slow repair rate. Upon the shift to increased light, the photoinactivation rate initially accelerated sharply (Fig. 8D), but the induction of PSII repair was slower and limited (Fig. 8D). Nevertheless, after 30 min of increased light, the photoinactivation rate fell back and was nearly countered by the PSII repair rate. Under increased light, a significant pool of intact but inactive PSIIi centers accumulated to about 9 fmol PSII $\mu g^{-1}$ protein, indicating that removal of inactivated protein subunits could be a rate-limiting step on the overall PSII repair cycle in *C. radiatus*, as supported by the lack of significant pools of disassembled PSII units. Overall, the allocation of total protein resources to PSII complexes and repair cycle intermediates was smaller in *C. radiatus*, largely through the absence of the large pools of inactive or disassembled PSII centers found in *T. pseudonana*. In both strains, clearance of PsbD under elevated light was comparable in magnitude and rate to the clearance of PsbA.

## DISCUSSION

In this study, we investigated how *T. pseudonana* and *C. radiatus* respond to the challenge of a shift from low growth light of 30 $\mu$mol $m^{-2}$ $s^{-1}$, approximating the bottom 10% of the photic zone, upward to the top third of the photic zone (450 $\mu$mol blue photons $m^{-2}$ $s^{-1}$) or to near-surface conditions (1,400 $\mu$mol $m^{-2}$ $s^{-1}$), approximating the top 7% of the photic zone. For these relatively moderate light-challenge experiments, we used a target size parameterization for primary susceptibility to photoinactivation of PSII (Nagy et al., 1995; Sinclair et al., 1996; Oliver et al., 2003) termed $\sigma_i$ (Six et al., 2007; Key et al., 2010). We find that, as expected, both *T. pseudonana* and *C. radiatus* show a larger $\sigma_i$ under BL than for RL (Table I; Supplemental Fig. S3, A and C), while treatment and growth temperature had little effect on susceptibility to primary photoinactivation under BL (Supplemental Fig. S3, B and D). This is consistent with the photoinactivation results and models of Hakala et al. (2005), Ohnishi et al. (2005), Sarvikas et al. (2006), and Tyystjarvi (2008), that under moderately high-light treatments the PSII photoinactivation is driven primarily, although not exclusively (Edelman and Mattoo, 2008), when BL directly photoinactivates PSII (Nishiyama et al., 2006). In the short term, within 15 to 30 min of a shift to a higher level of WL, the diatom responses were similar to an extrapolation upward from the moderate light response. After more extended exposure to higher WL, induction of a sustained phase of NPQs led to a continuing decline in the quantum yield of PSII, $F_v/F_m$, but a stabilization in the content of active PSII (Fig. 8), showing a photoprotective response to maintain a pool of down-regulated but functionally intact PSII units.

$\sigma_{PSII}$ and $\sigma_i$ are both target size parameterizations with units of area, and the ratio of $\sigma_{PSII}/|\sigma_i|$ approximates the ratio of exciton delivery to PSII to PSII photoinactivation (Table I). Under BL, *T. pseudonana* showed lower $\sigma_{PSII}/|\sigma_i|$ as compared with *C. radiatus* under BL, indicating fewer cycles of PSII photochemistry before photoinactivation, commensurate with the higher susceptibility to photoinactivation in the smaller cells of *T. pseudonana*.

If these diatoms mix rapidly from near the bottom of the photic zone to near the surface, they suffer an initial burn down in their content of active PSII units, which stabilizes through a combination of induction of PSII repair to rebuild active PSII and then induction of sustained NPQs to protect PSII content, albeit in a down-regulated state. The induction of PSII repair appears to saturate (Edelman and Mattoo, 2008) near the moderate light level of 450 $\mu$mol blue photons $m^{-2}$ $s^{-1}$, since the achieved PSII repair rate was slower under the higher WL treatment. During the light shift up to 1,400 $\mu$mol photons $m^{-2}$ $s^{-1}$, we observed strong induction of a sustained NPQs from 30 min onward, which coincided with a stabilization in the content of photochemically active, albeit down-regulated, PSII centers (compare Fig. 1, C and F, with Supplemental Fig. S2, C and F), supporting a photoprotective effect of NPQs induction, which allows the cells to retain a pool of intact but down-regulated PSII under high

light with only limited PSII repair. This induction of NPQs is consistent with the kinetics of induction of expression of the Lhcx6, Lhcx4, and Lhcx1 transcripts in *T. pseudonana* (Zhu and Green, 2010) under similar light treatments. These Lhcx genes are members of the LHC chlorophyll-binding protein superfamily and are implicated in modulating the induction of NPQ in diatoms (Bailleul et al., 2010). In contrast, induction of NPQs had only minor influence on the cellular response to the moderate light shift from 30 to 450 $\mu$mol red or blue photons $m^{-2} s^{-1}$, suggesting a two-phase response to light shifts, with initial acceleration of PSII repair followed by induction of NPQs if photoinactivation continues to outrun PSII repair.

We tracked MDA content as a proxy for cumulative peroxidation damage to membrane lipids by ROS. The MDA content was similar after the RL, BL, and WL treatments (Fig. 4), even though RL provoked much less photoinactivation than did the BL or high WL treatments in both species. We did observe a slowing of PSII repair under sustained high WL. Therefore, our results indicate that the enhanced photoinactivation under moderately high BL or high WL was not mediated through higher ROS toxicity, again consistent with Nishiyama et al. (2006) and Tyystjarvi (2008) and distinct from the results of Janknegt et al. (2009), who found that under yet higher full sunlight, differential ROS toxicity contributed significantly to differential photophysiology of phytoplankton taxa. We speculate that the induction of NPQs might preempt the production of ROS, although we have no direct evidence for this linkage as yet.

Turnover of the PsbA protein is generally required for PSII repair and the restoration of PSII photochemical activity after photoinactivation (Aro et al., 1993; Murata et al., 2007; Edelman and Mattoo, 2008; Nixon et al., 2010), although the kinetics and light responses of PsbA turnover and PSII repair are distinct (Edelman and Mattoo, 2008). Under increased light, *T. pseudonana* and *C. radiatus* were generally able to stabilize or even increase pools of PsbA protein when their repair cycle was active (Fig. 5). When lincomycin blocked the replacement of proteins, PsbA content dropped, although the patterns of decline differed across treatments and species. Similarly, PsbD content (Supplemental Fig. S4) dropped under BL and WL treatments in the presence of lincomycin, as did PsbB (Supplemental Fig. S5), although the variation among replicates was wider for PsbB.

Comparing changes in PsbA with changes in PSII function (Fig. 6) shows that under the BL and WL treatments, to mimic upward movement through an ocean light field, the drops in PSII activity approximately coincide with drops in PsbA content. PSII function often drops faster than PsbA content, suggesting a transient accumulation of intact but photoinactivated PsbA units. In contrast, upon the shift to increased RL, PsbA content dropped while PSII function was stable, particularly in *T. pseudonana*. The distinct patterns of PsbA content and PSII function under RL suggest a possible regulatory response (Edelman and Mattoo, 2008) in which increased RL provokes accelerated net clearance of PsbA from a pool of intact but previously photoinactivated PSII centers, present under low light in *T. pseudonana*.

Furthermore, in the smaller *T. pseudonana*, the initial content of 47 ± 9 fmol PsbA $\mu g^{-1}$ protein was much lower than the 121 ± 3 fmol PsbD $\mu g^{-1}$ protein. *C. radiatus* showed almost the same initial amounts of 23 ± 4 fmol PsbA $\mu g^{-1}$ protein versus 23 ± 1 fmol PsbD $\mu g^{-1}$ protein. Therefore, we have evidence of complexities in the PSII repair cycle, particularly in small diatoms, with significant pools of PSII subunits in excess of the equimolar ratios expected for assembled PSII complexes.

Previous studies with model cyanobacteria, green algae, and plants have found that the relative turnover rates of PSII protein subunits are as follows: D1 (PsbA) ≥ D2 (PsbD) > CP43 (PsbC) > CP47 (PsbB; Schuster et al., 1988; Jansen et al., 1999; Mattoo et al., 1999; Komenda et al., 2004; Yao et al., 2009). However, as Baroli and Melis (1996) found in *Dunaliella*, with diatoms under BL and WL, molar changes in PsbD content were similar in magnitude and in rate to changes in PsbA content (Fig. 7), albeit from higher starting PsbD contents in *T. pseudonana*. Accumulation of PsbD protein is a key regulatory step for assembly of the PSII reaction center complex, and it is hypothesized to act as a receptor component for newly synthesized PsbA protein (van Wijk et al., 1997; Komenda et al., 2004). The large excess content of PsbD in *T. pseudonana*, therefore, may represent a reserve pool of disassembled partial PSII centers, awaiting insertion of a PsbA unit, to support the maintenance of a functional pool of PSII (Fig. 8A), even while net content of the total PSII repair cycle intermediates is dropping. The fast turnover and accumulation of PsbD show further differences for PSII reaction center reassembly in the diatom chloroplasts compared with other organisms (Edelman and Mattoo, 2008; Nixon et al., 2010).

## CONCLUSION

In comparison with other taxonomic groups investigated under comparable conditions, including cyanobacteria and green alga (Six et al., 2007, 2009), these representative marine diatoms show a lower susceptibility to primary photoinactivation. The diatoms also show comparable turnover of both the PsbD and PsbA PSII subunits under multiple conditions, which was unexpected in comparison with most other taxa examined (Komenda and Masojídek, 1995; Jansen et al., 1996; Mattoo et al., 1999; Edelman and Mattoo, 2008; Nixon et al., 2010; but see Baroli and Melis, 1996). Furthermore, the smaller diatoms can rapidly modulate total PSII protein subunit content while maintaining a high PSII photochemical yield during moderate light shifts. The subunit stoi-

chiometries suggest that *T. pseudonana* maintains a pool of disassembled PSII lacking PsbA, which can receive nascent PsbA immediately upon synthesis. This rapid but costly strategy could mitigate limitations on repair cycles that rely upon initial removal of photodamaged PsbA by proteolysis. Under sustained excess light, the diatoms then induce a photoprotective NPQs (Nymark et al., 2009; Zhu and Green, 2010) to inexpensively maintain a pool of intact but downregulated PSII using only moderate sustained repair rates. These distinct mechanistic aspects of the diatom chlorophyll *a*/*c* chloroplast PSII repair cycle help explain their successful exploitation of variable light environments.

## MATERIALS AND METHODS

### Culture Conditions and High-Light Treatments

The diatoms *Thalassiosira pseudonana* CCMP 1014 and *Coscinodiscus radiatus* CCMP 312 (both obtained from the Provasoli-Guillard National Center for Culture of Marine Phytoplankton) were grown in semicontinuous batch cultures using K medium (Keller et al., 1987) in polystyrene flasks (Corning) at 12°C (for *T. pseudonana* only), 18°C, and 24°C. Continuous light of 30 $\mu$mol photons $m^{-2}$ $s^{-1}$ provided by fluorescent tubes (Sylvania) was used and measured in the culture flasks by a microspherical quantum sensor (US-SQS; Walz) connected to a Li-Cor quantumeter (LI-250). The cultures were agitated manually twice daily. Cell densities were monitored by cell counts using a Beckman counter (Multisizer 3) for *T. pseudonana* CCMP 1014 and using a Sedwick-Rafter counting chamber with a light microscope for *C. radiatus* CCMP 312.

Culture replicates from the exponential growth phase were split into two flasks, with 500 $\mu$g $mL^{-1}$ lincomycin added to one flask to block chloroplast protein synthesis (Bachmann et al., 2004), thereby inhibiting PSII repair (Baroli and Melis, 1996; Tyystjärvi and Aro, 1996). Both flasks were incubated in the dark for 10 min to allow the lincomycin to exert its effect and then placed at 18°C under RL (LEE Filter no. 183; 455- to 479-nm peak transmission, 406- to 529-nm half-height width) or BL (LEE Filter no. 026; 680- to 700-nm peak transmission, 620- to 700-nm half-height width) of 450 $\mu$mol photons $m^{-2}$ $s^{-1}$, or WL of 1,400 $\mu$mol photons $m^{-2}$ $s^{-1}$, provided by fluorescent tubes for 90 min. Samples were collected prior to the onset of high light (plotted as time 0) and 15, 30, 60, and 90 min for chlorophyll fluorescence analyses and for filtration onto glass fiber filters, which were flash frozen for later protein immunoblotting, pigment, and ROS product analyses. Following the high-light treatment, the remaining cultures were returned to their initial growth light of 30 $\mu$mol photons $m^{-2}$ $s^{-1}$ for a 30-min recovery period followed by terminal sampling.

### Fluorescence Measurement and Photoinactivation Parameterization

Chlorophyll fluorescence yield data were collected using a Xe-PAM fluorometer (Walz) connected to a temperature-controlled cuvette holder (Walz). At each sampling point, a sample of culture was dark adapted for 5 min to relax photosynthetic activity. The modulated (4-Hz) BL measuring beam was used to measure $F_0$, followed by a saturating WL pulse (4,000 $\mu$mol photons $m^{-2}$ $s^{-1}$) to measure $F_m$ (dark). The maximum quantum yield of PSII photochemistry was then estimated as $F_v/F_m = (F_m - F_0)/F_m$.

Two kinetic components of NPQ were estimated. Dynamic NPQ, which relaxed within the 5-min dark period before measurement and was then reinduced within the short measuring period, was estimated as NPQd = $(F_m - F_m')/F_m'$.

Any sustained phase of NPQ that was induced over the course of the high-light treatment and that persisted through the 5-min dark acclimation period just before measurement was estimated as NPQs = $(F_{mt0} - F_m)/F_m$.

$F_{mt0}$ is the measurement of $F_m$ from dark-acclimated cells taken at time 0 (t0) just before the start of high-light treatment. $F_m$ is taken at each measurement time point during the high-light treatment. NPQs by definition thus starts at 0 at time 0 and increases if the cells accumulate a sustained phase of NPQ. To separate the effects of sustained components of NPQ from the effects of photoinactivation and PSII repair, we used $1/F_0 - 1/F_m$, arithmetically equivalent to division of $F_v/F_m$ by $F_0$ (Havaux et al., 1991; Park et al., 1995; Lee et al., 1999; He and Chow, 2003) and linearly correlated to the content of functional PSII.

$F_v/F_m$ and $1/F_0 - 1/F_m$ were plotted over time for both the control and lincomycin-treated subcultures. Using $1/F_0 - 1/F_m$, an exponential decay curve was fitted over the high-light treatment period for the +lincomycin cultures to estimate the irradiance-specific rate constant for photoinactivation, $k_\pi$ (Kok, 1956; Oliver et al., 2003). We generalize $k_\pi$ to an effective target size for primary PSII photoinactivation (Nagy et al., 1995; Sinclair et al., 1996; Six et al., 2007, 2009; Key et al., 2010) termed $\sigma_i$ ($Å^2$ $quanta^{-1}$), arithmetically equivalent to $k_\pi$ ($s^{-1}$) divided by E (photons $A^{-2}$ $s^{-1}$; Oliver et al., 2003), and estimated as the exponential decay for $1/F_0 - 1/F_m$ in the absence of PSII repair, plotted versus cumulative incident photons, and measured with a microspherical quantum sensor in the cell culture. The $\sigma_i$ parameter does not represent the physical size of a target molecule or atom. Instead, in units of area, it folds together the probability of absorbance of the photon with the probability that the absorbance event provokes the measured response, a drop in $1/F_0 - 1/F_m$ (or $F_v/F_m$).

The functional absorption cross section serving PSII photochemistry ($\sigma_{PSII}$ [$Å^2$ $quanta^{-1}$]; Falkowski and Raven, 1997) was determined on a culture sample dark acclimated for 5 min and then exposed to a saturating single-turnover flash (BL-emitting diode, 455 ± 20 nm; FIRe fluorometer; Satlantic). Values of $\sigma_{PSII}$ were determined from the fluorescence saturation curves analyzed with MATLAB software using the Fireworx program (Barnett, 2007), with instrument-specific light calibration factors (Satlantic).

### Quantitation of Proteins by Immunoblotting

Cells were harvested on glass fiber filters (25 mm diameter; binder-free glass fiber; Whatman), which were immediately flash frozen in liquid nitrogen and stored at −80°C for later protein analyses by quantitative immunoblotting. In particular, we quantified molar levels of PsbA (D1), PsbD (D2), and PsbB (CP47) from samples taken during the high-light treatment time courses. Total proteins were extracted by two thawing/sonicating rounds in denaturing extraction buffer (Brown et al., 2008). The total protein concentration was determined (Lowry protein assay kit; Bio-Rad-DC Assay). One microgram of total protein was loaded on a 4% to 12% acrylamide precast NuPAGE gel (Invitrogen). Along with the samples, protein standards for each target protein (AgriSera; www.agrisera.se) were loaded to establish a standard curve. Electrophoresis was run for 40 min at 200 V, and the proteins were transferred to a polyvinylidene difluoride membrane. After membrane blocking, primary antibody against the C-terminal part of PsbA (AgriSera; 1:50,000), PsbD (AgriSera; 1:50,000), or PsbB (AgriSera; 1:10,000) were applied, followed by an anti-rabbit secondary antibody coupled with horseradish peroxidase. The membranes were developed by chemiluminescence using ECL Advance (Amersham Biosciences) and a CCD imager (Kodak 4000MMPro; Carestream). Target protein concentrations were determined by fitting the sample signal values to the protein standard curves, taking care that all sample signals fell within the range of the protein standard curve and that no band signals were saturated.

### Measurement of ROS-Induced Lipid Peroxidation Products

Lipid peroxidation was measured as the amount of MDA accumulated as an index of cumulative ROS toxicity. MDA content was determined using the thiobarbituric acid-reactive substance method (Heath and Packer, 1968; Hong et al., 2008; Janknegt et al., 2008). Samples were collected by membrane filtration as for protein analyses, at time 0 and 90 min of high-light treatment and at the subsequent 30-min recovery point, and were immediately flash frozen in liquid nitrogen and stored at −80°C for later MDA content analysis. Cells were homogenized with 1.2 mL of 20% (w/v) TCA. The homogenate was then centrifuged at 13,000*g* for 10 min, and the supernatant was reserved. A total of 0.45 mL of the supernatant and 0.45 mL of thiobarbituric acid reagent (0.5% in 20% TCA) were mixed and heated for 30 min at 90°C, then cooled, and the absorbance of the supernatants was read at 532 nm. MDA contents were calculated based on $A_{532} - A_{600}$ with the extinction coefficient of 155 $mM^{-1}$ $cm^{-1}$.

## Supplemental Data

The following materials are available in the online version of this article.

**Supplemental Figure S1.** Responses of rapidly reversible, dynamic NPQ versus time in *T. pseudonana* and *C. radiatus* treated with or without the chloroplast protein synthesis inhibitor lincomycin to block PSII repair.

**Supplemental Figure S2.** Responses of PSII photoinhibition ($1/F_0 - 1/F_m$) versus time in *T. pseudonana* and *C. radiatus* treated with or without the chloroplast protein synthesis inhibitor lincomycin to block PSII repair.

**Supplemental Figure S3.** Responses of PSII photoinhibition ($1/F_0 - 1/F_m$) as a function of cumulative incident photons per area for *T. pseudonana* and *C. radiatus* in the presence of lincomycin to block PSII repair.

**Supplemental Figure S4.** Changes in PsbD content in *T. pseudonana* and *C. radiatus* treated with or without the chloroplast protein synthesis inhibitor lincomycin.

**Supplemental Figure S5.** Changes in PsbB content in *T. pseudonana* and *C. radiatus* treated with or without the chloroplast protein synthesis inhibitor lincomycin.

## ACKNOWLEDGMENTS

We thank Laurel McIntyre for assistance with cell culturing; Natalie Donaher for assistance with protein immunoquantitations; and Drs. Esa Tyystjärvi, Zoe Finkel, Hugh MacIntyre, Dave Suggett, and Benjamin Bailleul for productive discussions.

Received April 21, 2011; accepted May 24, 2011; published May 26, 2011.

## LITERATURE CITED

**Armbrust EV, Berges JA, Bowler C, Green BR, Martinez D, Putnam NH, Zhou S, Allen AE, Apt KE, Bechner M, et al** (2004) The genome of the diatom Thalassiosira pseudonana: ecology, evolution, and metabolism. Science **306:** 79–86

**Aro EM, Suorsa M, Rokka A, Allahverdiyeva Y, Paakkarinen V, Saleem A, Battchikova N, Rintamäki E** (2005) Dynamics of photosystem II: a proteomic approach to thylakoid protein complexes. J Exp Bot **56:** 347–356

**Aro EM, Virgin I, Andersson B** (1993) Photoinhibition of photosystem II: inactivation, protein damage and turnover. Biochim Biophys Acta **1143:** 113–134

**Bachmann KM, Ebbert V, Adams WW, Verhoeven AS, Logan BA, Demmig-Adams B** (2004) Effects of lincomycin on PSII efficiency, non-photochemical quenching, D1 protein and xanthophyll cycle during photoinhibition and recovery. Funct Plant Biol **31:** 803–813

**Bailleul B, Rogato A, de Martino A, Coesel S, Cardol P, Bowler C, Falciatore A, Finazzi G** (2010) An atypical member of the light-harvesting complex stress-related protein family modulates diatom responses to light. Proc Natl Acad Sci USA **107:** 18214–18219

**Barnett AB** (2007) Fireworx 1.0.3. Dalhousie University, Halifax, Canada. http://sourceforge.net/projects/fireworx (May 15, 2010)

**Baroli I, Melis A** (1996) Photoinhibition and repair in Dunaliella salina acclimated to different growth irradiances. Planta **198:** 640–646

**Beardall J, Allen D, Bragg J, Finkel ZV, Flynn KJ, Quigg A, Rees TA, Richardson A, Raven JA** (2009) Allometry and stoichiometry of unicellular, colonial and multicellular phytoplankton. New Phytol **181:** 295–309

**Bowler C, Vardi A, Allen AE** (2010) Oceanographic and biogeochemical insights from diatom genomes. Annu Rev Mar Sci **2:** 333–365

**Brown CM, MacKinnon JD, Cockshutt AM, Villareal T, Campbell DA** (2008) Flux capacities and acclimation costs in Trichodesmium from the Gulf of Mexico. Mar Biol **154:** 413–422

**Campbell D, Tyystjärvi E** (May 1, 2011) Parameterization of photosystem II photoinactivation and repair. Biochim Biophys Acta http://dx.doi.org/10.1016/j.bbabio.2011.04.010

**Critchley C, Russell AW, Bolhar-Nordenkampf HR** (1992) Rapid protein-turnover in photosystem-2: fundamental flaw or regulatory mechanism. Photosynthetica **27:** 183–190

**de Vitry C, Olive J, Drapier D, Recouvreur M, Wollman FA** (1989) Posttranslational events leading to the assembly of photosystem II protein complex: a study using photosynthesis mutants from Chlamydomonas reinhardtii. J Cell Biol **109:** 991–1006

**Edelman M, Mattoo AK** (2008) D1-protein dynamics in photosystem II: the lingering enigma. Photosynth Res **98:** 609–620

**Eisenstadt D, Ohad I, Keren N, Kaplan A** (2008) Changes in the photosynthetic reaction centre II in the diatom Phaeodactylum tricornutum result in non-photochemical fluorescence quenching. Environ Microbiol **10:** 1997–2007

**Falkowski P, Raven JA** (1997) Aquatic Photosynthesis. Blackwell Science, Oxford

**Field CB, Behrenfeld MJ, Randerson JT, Falkowski P** (1998) Primary production of the biosphere: integrating terrestrial and oceanic components. Science **281:** 237–240

**Grouneva I, Jakob T, Wilhelm C, Goss R** (2009) The regulation of xanthophyll cycle activity and of non-photochemical fluorescence quenching by two alternative electron flows in the diatoms Phaeodactylum tricornutum and Cyclotella meneghiniana. Biochim Biophys Acta **1787:** 929–938

**Hakala M, Tuominen I, Keränen M, Tyystjärvi T, Tyystjärvi E** (2005) Evidence for the role of the oxygen-evolving manganese complex in photoinhibition of photosystem II. Biochim Biophys Acta **1706:** 68–80

**Havaux M, Strasser RJ, Greppin H** (1991) A theoretical and experimental analysis of the qP and qN coefficients of chlorophyll fluorescence quenching and their relation to photochemical and nonphotochemical events. Photosynth Res **27:** 41–55

**He J, Chow WS** (2003) The rate coefficient of repair of photosystem II after photoinactivation. Physiol Plant **118:** 297–304

**Heath RL, Packer L** (1968) Photoperoxidation in isolated chloroplasts. I. Kinetics and stoichiometry of fatty acid peroxidation. Arch Biochem Biophys **125:** 189–198

**Hong Y, Hu HY, Li FM** (2008) Growth and physiological responses of freshwater green alga Selenastrum capricornutum to allelochemical ethyl 2-methyl acetoacetate (EMA) under different initial algal densities. Pestic Biochem Physiol **90:** 203–212

**Janknegt P, de Graaff M, van de Poll W, Visser R, Rijstenbil J, Buma A** (2009) Short term antioxidative response of 15 microalgae exposed to excessive irradiance including unltraviolet radiation. Eur J Phycol **44:** 525–539

**Janknegt PJ, van de Poll WH, Visser RJW, Rijstenbil JW, Buma AGJ** (2008) Oxidative stress responses in the marine Antarctic diatom Chaetoceros brevis (Bacillariophyceae) during photoacclimation. J Phycol **44:** 957–966

**Jansen MAK, Greenberg BM, Edelman M, Mattoo AK, Gaba V** (1996) Accelerated degradation of the D2 protein of photosystem-II under ultraviolet-radiation. Photochem Photobiol **63:** 814–817

**Jansen MAK, Mattoo AK, Edelman M** (1999) D1-D2 protein degradation in the chloroplast: complex light saturation kinetics. Eur J Biochem **260:** 527–532

**Keller MD, Selvin RC, Claus W, Guillard RRL** (1987) Media for the culture of oceanic ultraphytoplankton. J Phycol **23:** 633–638

**Key T, McCarthy A, Campbell DA, Six C, Roy S, Finkel ZV** (2010) Cell size trade-offs govern light exploitation strategies in marine phytoplankton. Environ Microbiol **12:** 95–104

**Kim JH, Nemson JA, Melis A** (1993) Photosystem II reaction center damage and repair in *Dunaliella salina* (green alga): analysis under physiological and irradiance-stress conditions. Plant Physiol **103:** 181–189

**Komenda J, Masojídek J** (1995) Functional and structural changes of the photosystem II complex induced by high irradiance in cyanobacterial cells. Eur J Biochem **233:** 677–682

**Komenda J, Reisinger V, Müller BC, Dobáková M, Granvogl B, Eichacker LA** (2004) Accumulation of the D2 protein is a key regulatory step for assembly of the photosystem II reaction center complex in Synechocystis PCC 6803. J Biol Chem **279:** 48620–48629

**Kok B** (1956) On the inhibition of photosynthesis by intense light. Biochim Biophys Acta **21:** 234–244

**Larkum AWD, Lockhart PJ, Howe CJ** (2007) Shopping for plastids. Trends Plant Sci **12:** 189–195

**Lavaud J, Rousseau B, Etienne AL** (2004) General features of photoprotection by energy dissipation in planktonic diatoms (Bacillariophyceae). J Phycol **40:** 130–137

**Lee H-Y, Chow WS, Hong Y-N** (1999) Photoinactivation of photosystem II in leaves of Capsicum annuum. Physiol Plant **105:** 377–384

**Long S, Humphries S, Falkowski P** (1994) Photoinhibition of photosynthesis in nature. Annu Rev Plant Physiol Plant Mol Biol **45:** 633–662

**MacIntyre HL, Kana TM, Geider RJ** (2000) The effect of water motion on short-term rates of photosynthesis by marine phytoplankton. Trends Plant Sci **5:** 12–17

**Mattoo AK, Giardi MT, Raskind A, Edelman M** (1999) Dynamic metabolism of photosystem II reaction center proteins and pigments. Physiol Plant **107:** 454–461

**Medlin LK, Kaszmarska I** (2004) Evolution of diatoms. V. Morphological and cytological support for the major clades and a taxonomic revision. Phycologia **43:** 245–270

**Müller P, Li XP, Niyogi KK** (2001) Non-photochemical quenching: a response to excess light energy. Plant Physiol **125:** 1558–1566

**Murata N, Takahashi S, Nishiyama Y, Allakhverdiev SI** (2007) Photoinhibition of photosystem II under environmental stress. Biochim Biophys Acta **1767:** 414–421

**Nagy L, Balint E, Barber J, Ringler A, Cook KM, Maroti P** (1995) Photoinhibition and law of reciprocity in photosynthetic reactions of Synechocystis sp. PCC 6803. J Plant Physiol **145:** 410–444

**Nishiyama Y, Allakhverdiev SI, Murata N** (2005) Inhibition of the repair of photosystem II by oxidative stress in cyanobacteria. Photosynth Res **84:** 1–7

**Nishiyama Y, Allakhverdiev SI, Murata N** (2006) A new paradigm for the action of reactive oxygen species in the photoinhibition of photosystem II. Biochim Biophys Acta **1757:** 742–749

**Nixon PJ, Michoux F, Yu J, Boehm M, Komenda J** (2010) Recent advances in understanding the assembly and repair of photosystem II. Ann Bot (Lond) **106:** 1–16

**Nymark M, Valle KC, Brembu T, Hancke K, Winge P, Andresen K, Johnsen G, Bones AM** (2009) An integrated analysis of molecular acclimation to high light in the marine diatom Phaeodactylum tricornutum. PLoS ONE **4:** e7743

**Ohnishi N, Allakhverdiev SI, Takahashi S, Higashi S, Watanabe M, Nishiyama Y, Murata N** (2005) Two-step mechanism of photodamage to photosystem II: step 1 occurs at the oxygen-evolving complex and step 2 occurs at the photochemical reaction center. Biochemistry **44:** 8494–8499

**Oliver RL, Whittington J, Lorenz Z, Webster IT** (2003) The influence of vertical mixing on the photoinhibition of variable chlorophyll a fluorescence and its inclusion in a model of phytoplankton photosynthesis. J Plankton Res **25:** 1107–1129

**Park S, Jung G, Hwang YS, Jin ES** (2010) Dynamic response of the transcriptome of a psychrophilic diatom, Chaetoceros neogracile, to high irradiance. Planta **231:** 349–360

**Park Y-I, Chow WS, Anderson JM** (1995) Light inactivation of functional photosystem II in leaves of peas grown in moderate light depends on photon exposure. Planta **196:** 401–411

**Sarvikas P, Hakala M, Pätsikkä E, Tyystjärvi T, Tyystjärvi E** (2006) Action spectrum of photoinhibition in leaves of wild type and npq1-2 and npq4-1 mutants of Arabidopsis thaliana. Plant Cell Physiol **47:** 391–400

**Schuster G, Timberg R, Ohad I** (1988) Turnover of thylakoid photosystem II proteins during photoinhibition of Chlamydomonas reinhardtii. Eur J Biochem **177:** 403–410

**Silva P, Thompson E, Bailey S, Kruse O, Mullineaux CW, Robinson C, Mann NH, Nixon PJ** (2003) FtsH is involved in the early stages of repair of photosystem II in *Synechocystis* sp PCC 6803. Plant Cell **15:** 2152–2164

**Sinclair J, Park YI, Chow WS, Anderson JM** (1996) Target theory and the photoinactivation of photosystem II. Photosynth Res **50:** 33–40

**Six C, Finkel ZV, Irwin AJ, Campbell DA** (2007) Light variability illuminates niche-partitioning among marine picocyanobacteria. PLoS ONE **2:** e1341

**Six C, Sherrard R, Lionard M, Roy S, Campbell DA** (2009) Photosystem II and pigment dynamics among ecotypes of the green alga *Ostreococcus*. Plant Physiol **151:** 379–390

**Sundby C, McCaffery S, Anderson JM** (1993) Turnover of the photosystem II D1 protein in higher plants under photoinhibitory and nonphotoinhibitory irradiance. J Biol Chem **268:** 25476–25482

**Tyystjarvi E** (2008) Photoinhibition of photosystem II and photodamage of the oxygen evolving manganese cluster. Coord Chem Rev **252:** 361–376

**Tyystjärvi E, Aro EM** (1996) The rate constant of photoinhibition, measured in lincomycin-treated leaves, is directly proportional to light intensity. Proc Natl Acad Sci USA **93:** 2213–2218

**van Wijk KJ, Roobol-Boza M, Kettunen R, Andersson B, Aro EM** (1997) Synthesis and assembly of the D1 protein into photosystem II: processing of the C-terminus and identification of the initial assembly partners and complexes during photosystem II repair. Biochemistry **36:** 6178–6186

**Wilhelm C, Büchel C, Fisahn J, Goss R, Jakob T, Laroche J, Lavaud J, Lohr M, Riebesell U, Stehfest K, et al** (2006) The regulation of carbon and nutrient assimilation in diatoms is significantly different from green algae. Protist **157:** 91–124

**Yao D, Brune D, Vermaas WFJ** (2009) Photosystem II protein lifetimes in vivo in Synechocystis. *In* OC-6.2, International Symposium on Phototrophic Prokaryotes, Montreal. ISPP, Montreal, p 58

**Yu J, Vermaas WFJ** (1990) Transcript levels and synthesis of photosystem II components in cyanobacterial mutants with inactivated photosystem II genes. Plant Cell **2:** 315–322

**Zhang LX, Paakkarinen V, van Wijk KJ, Aro EM** (1999) Co-translational assembly of the D1 protein into photosystem II. J Biol Chem **274:** 16062–16067

**Zhu SH, Green BR** (2010) Photoprotection in the diatom Thalassiosira pseudonana: role of LI818-like proteins in response to high light stress. Biochim Biophys Acta **1797:** 1449–1457